JOURNAL OF SOLID STATE CHEMISTRY 111, 151–156 (1994)

Sorbate Properties of Xenon in Cloverite: A Molecular Dynamics Study[1]

Sanjoy Bandyopadhyay* and Subramanian Yashonath*†[2]

*Solid State and Structural Chemistry Unit and †Supercomputer Education and Research Centre, Indian Institute of Science, Bangalore-560012, India

Received November 10, 1993; accepted January 13, 1994

IN HONOR OF C. N. R. RAO ON HIS 60TH BIRTHDAY

Molecular dynamics calculations on xenon adsorbed in the cubic cavity of cloverite, a gallophosphate, is presented. Guest–host radial distribution functions, guest–host energy distribution functions, power spectra, and diffusion coefficients for xenon are reported at 397, 494, and 716 K. Results suggest that xenon is highly mobile at 700 K. A shift in the peak position of the power spectra toward lower frequency is observed with increase in temperature. © 1994 Academic Press, Inc.

1. INTRODUCTION

In recent times molecular recognition has been found to play an important role in several branches of chemistry (1). A number of organic as well as inorganic materials having porous structures exhibit the molecular recognition property (2). Among the inorganic solids zeolites are one of the important materials which belong to this class (3). In addition, zeolites exhibit catalytic properties. However, most zeolites have rather small pore dimensions (up to 13 Å). Recent work on alternatives to zeolites suggest that gallophosphates such as cloverite could have considerably larger pore dimensions (29–30 Å) (4). Availability of hosts with such large pore dimension is important in a number of areas such as encapsulation of semiconductor nanoclusters and *in situ* reactions of bigger molecules. Recent work by Bedard *et al.* (5) suggests the possibility of using cloverite for advanced materials science applications. In order to exploit cloverite for such applications it is necessary to understand the adsorption properties including thermodynamic, structural, and dynamical properties of the sorbate in its cages and channels. In this work we report a molecular dynamics investigation of xenon sorbed in cloverite. We have chosen xenon since it is important to understand the diffusion of simple monatomic sorbates before one can investigate molecules of complicated geometries.

2. STRUCTURE OF CLOVERITE AND INTERMOLECULAR POTENTIAL FUNCTIONS

The structure of cloverite obtained recently from high-resolution synchrotron powder diffraction by Estermann *et al.* (4) has been used in this study. The space group is $Fm\bar{3}c$. The lattice parameter of bare cloverite with $a = 52.712$ Å has been employed. One unit cell has 768 gallium, 768 phosphorous, and 2976 oxygen atoms and 192 terminal hydroxyl groups. The framework structure consists of α cages interconnected along the edges of the crystallographic unit cell by two rpa cages (see Fig. 1). Such an arrangement leads to a cubic supercage at the center whose dimension along the body diagonal is 29–30 Å. This may be compared with supercages in faujasites whose dimensions are in the range 11.5–12.5 Å. The overall structure has two nonintersecting three-dimensional channel systems. One of these extends through α and rpa cages. The smallest diameter of this channel occurs at the eight ring window whose diameter is 3.8 Å (5). The other channel has a cloverleaf-shaped opening at the center of the face of the crystallographic unit cell. This window is made up of 20 tetrahedral atoms (Ga and P) and 24 oxygens and has an approximate diameter of about 6 Å (4). The unusual cloverleaf shape of the window is due to the presence of the terminal OH groups which protrude into the window. The two channel systems are nonintersecting. However, it is possible for a sufficiently small sized guest in one channel to enter the other channel via the six T-atom rings. Xenon was introduced at the beginning of the simulation in the larger channel system located at the face center position. Since the six-membered ring interconnecting the two channel systems is too small for xenon, the motion of the sorbate

[1] Contribution No. 967 from the Solid State and Structural Chemistry Unit.

[2] To whom correspondence should be addressed.

0022-4596/94 $6.00

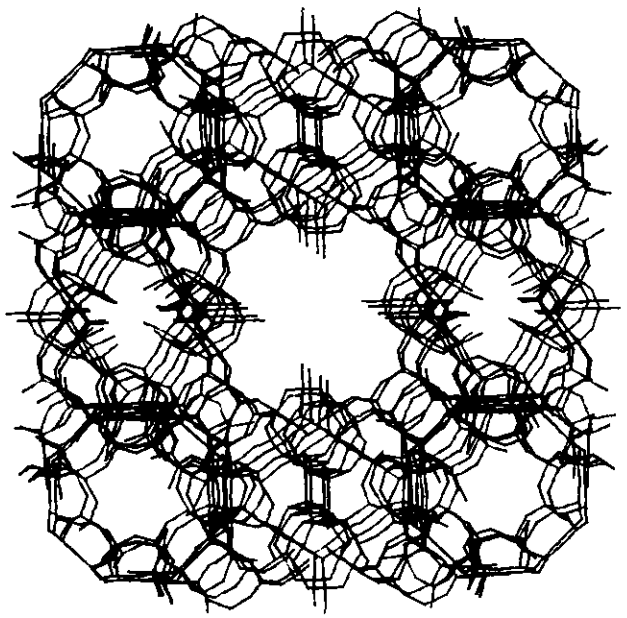

FIG. 1. One crystallographic unit cell of cloverite, a gallophosphate, consisting of α cages interconnected by two rpa cages along the edges is shown. A large cubic supercage of 29–30 Å in length along the body diagonal may be seen at the center of the unit cell. Properties of xenon adsorbed in this supercage are investigated.

was restricted to this larger channel system. Hence all the properties obtained here are for the motion of xenon in this channel system.

All guest–zeolite interactions were modeled in terms of short-range interactions using atom–atom pair potentials. The interactions between xenon and oxygen and hydroxyl groups of the zeolite framework were modeled in terms of the (6–12) Lennard–Jones potential

$$\phi_{az}(r_{az}) = -A_{az}/r_{az}^6 + B_{az}/r_{az}^{12}, \quad a = \text{Xe and } z = \text{O, OH}, \tag{1}$$

where $A_{az} = 4\varepsilon_{az}\sigma_{az}^6$ and $B_{az} = 4\varepsilon_{az}\sigma_{az}^{12}$. The interaction between gallium or phosphorous and xenon were taken to be zero as the close approach of xenons to these atoms is prevented by the surrounding oxygens. This approximation has been found to be acceptable (6–8). Potential parameter values for xenon–oxygen interactions obtained for faujasite by Kiselev and Du has been adopted here without any modification (9). The self-interaction parameters σ and ε of the hydroxyl group were taken from the work on alcohol of Jorgensen (10). The interaction parameters between xenon and the hydroxyl group were then obtained using the Lorentz–Berthelot mixing rules (11). The potential parameters are listed in Table 1.

The xenon–xenon interactions were taken to be of the Lennard–Jones (6–12) form. The values of $\varepsilon_{Xe\text{-}Xe} = 221$ K and $\sigma_{Xe\text{-}Xe} = 4.1$ Å were taken from the literature (7). The atomic mass of xenon was taken to be 131 amu.

TABLE 1
Intermolecular Potential Parameters for Guest–Guest and Guest–Zeolite Interactions

Atom	$A(10^3$ kJ/mole, Å^6)	$B(10^6$ kJ/mole, Å^{12})
Guest–guest		
Xe–Xe	34.911	165.832
Guest–zeolite		
Xe–O	8.279	11.134
Xe–OH	9.921	21.288

3. COMPUTATIONAL DETAILS

All calculations were carried out in the microcanonical ensemble at fixed (N, V, E). Cubic periodic boundary conditions were employed. The zeolite atoms were assumed to be rigid and were not included in the integration. The integration of the sorbate atoms was carried out using the Verlet scheme. Calculations were performed at three different temperatures with 25 sorbate particles. At all temperatures the sorbate particles were placed in the larger three-dimensional channel system. One unit cell of cloverite was employed in all calculations. A time step of 20 fs and a fairly large spherical cutoff of 20 Å for guest–guest and guest–host interactions have been employed. These yielded good energy conservation. Properties were calculated from configurations stored at intervals of 0.2 ps. Equilibration was performed over a duration of 200 ps during which velocities were scaled to obtain the desired temperature. Production runs were of 500 ps duration at all temperatures.

4. RESULTS AND DISCUSSIONS

4.1. Structure and Energetics

Thermodynamic properties for xenon in cloverite at different temperatures are listed in Table 2. The guest–

TABLE 2
Equilibrium Thermodynamic Properties for Xenon in Cloverite at Different Temperatures

$\langle T \rangle$ (K)	$\langle U_{gg} \rangle$ (kJ/mole)	$\langle U_{gh} \rangle$ (kJ/mole)	$\langle U \rangle$ (kJ/mole)	q_{st} (kJ/mole)
397	−3.21	−16.03	−19.24	22.54
494	−2.24	−14.77	−17.01	21.12
716	−2.78	−12.38	−15.16	21.1

host interaction energy, U_{gh}, decreases with increase in temperature. No such trend is visible in the case of guest–guest interaction energy, U_{gg}. The total energy, U, as well as the isosteric heat of adsorption, q_{st}, are also listed. Due to the nonavailability of experimental data we are unable to compare these results with any measurements.

Figure 2 shows a plot of the guest–host radial distribution function for Xe–O, Xe–OH, and Xe–P/Ga for three different temperatures. It is seen that at lower temperatures the main peak in the Xe–OH radial distribution function is around 8 Å. This peak reduces in intensity with increase in temperature. This is simultaneously accompanied by an increase in intensity of the peak near 4 Å. At lower temperatures xenon is significantly localized near the adsorption site. The location of the adsorption site is shown in Fig. 3. The adsorption site is in the pocket located near the vertices of the cubic-shaped cavity as is evident from the figure. The pocket is at a considerable distance from the OH group which is responsible for the 8-Å peak at lower temperatures. Increasing the temperature results in xenon becoming more delocalized. This leads to an increase in intensity of the peak near 4 Å. The delocalization of xenon with increase in temperature is also evident from the decrease in the intensity of Xe–O as well as Xe–P/Ga radial distribution functions. The comparatively higher intensity of Xe–OH peaks arise from the fact that there are much fewer OH groups than O and P/Ga atoms and that the OH groups are located at only specific positions inside the cage. A similar observation has been made for xenon adsorbed in zeolite NaY (7) where the peaks in the Xe–Na radial distribution function were found to be more intense than those in the Xe–O and Xe–Si/Al functions.

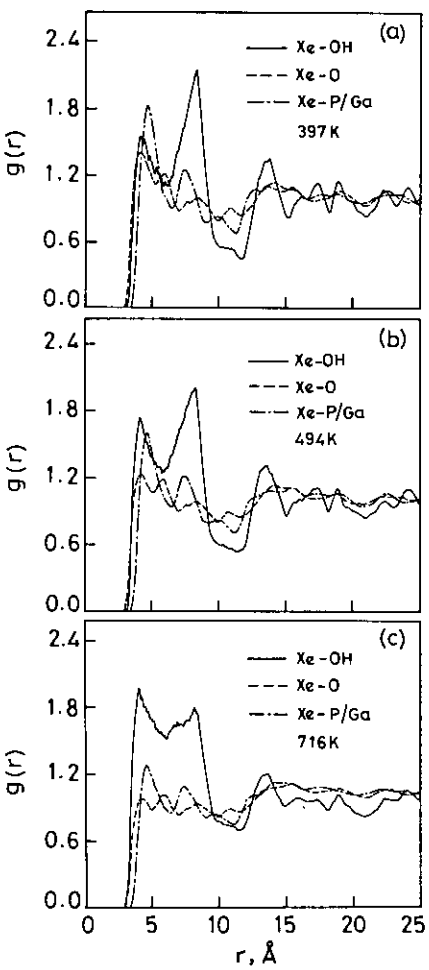

FIG. 2. Guest–host radial distribution functions between xenon and oxygen, the hydroxyl group, and phosphorous or gallium is shown at (a) 397, (b) 494, and (c) 716 K.

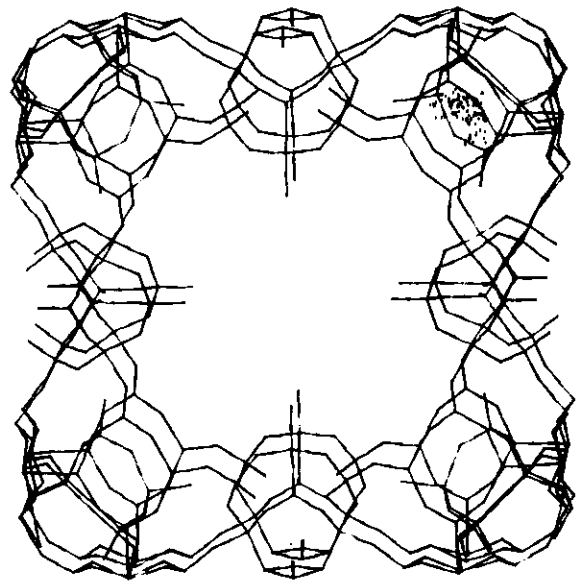

FIG. 3. A short molecular dynamics trajectory of xenon at the adsorption site. The calculation was carried out at 275 K. The guest–host interaction energy was around −24 kJ/mol.

The distribution function for the guest–host interaction energy, $f(U_{gh})$, is shown in Fig. 4. At low temperature a significant population of the guest interact strongly with the zeolite framework, $U_{gh} \simeq -24$ kJ/mol. This peak reduces in intensity significantly only when the temperature is raised beyond 494 K to 716 K. This reduction is accompanied by a reduction in intensity of the peak around −14 kJ/mol. This reduction in the two peaks is accompanied by an increase in intensity in the region between 0 and −10 kJ/mol. At 716 K a new peak begins to appear around −6 kJ/mol. This peak may be attributed to highly delocalized xenon. Similar trends were observed in the case of zeolites Y and A (7, 12).

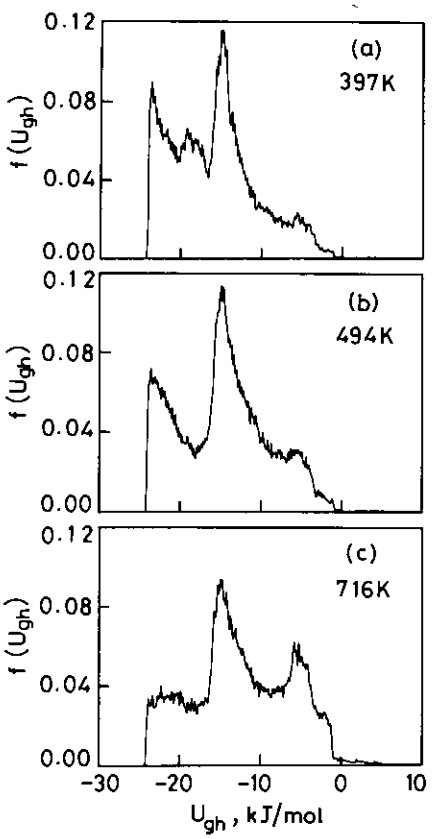

FIG. 4. Guest–host energy distribution function at different temperatures.

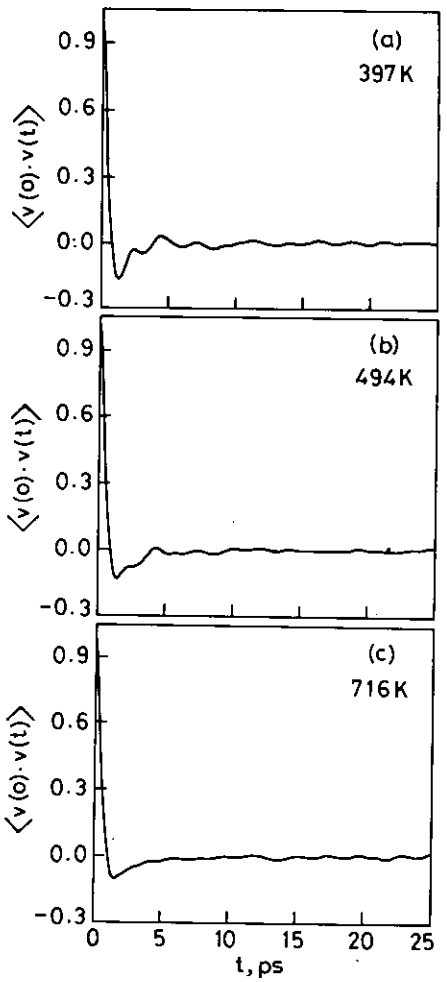

FIG. 5. Velocity autocorrelation function for xenon sorbed in cloverite at different temperatures.

4.2. Dynamical Properties

Figure 5 shows a plot of the velocity autocorrelation function for the three temperatures. At 397 K the velocity autocorrelation function suggests that the particle is encountering frequent collisions. By 716 K the nature of the calculated velocity autocorrelation function suggests essentially free motion of the xenon. Fourier transform of the velocity autocorrelation function is shown in Fig. 6. A single broad peak extending between 5 and 20 cm^{-1} is observed at 397 K. At higher temperatures there is a reduction in the intensity beyond 10 cm^{-1}. Simultaneously there is a shift of the peak toward lower frequency. We attribute the peak around 13 cm^{-1} in the power spectra at 397 and 494 K to the vibration of xenon trapped in the adsorption site shown in Fig. 3.

The variation of the mean-square displacement $\langle u^2(t)\rangle$ with time is shown in Fig. 7. It is clear from the figure that at 397 and 494 K xenon undergoes significantly less displacement than at 716 K. This is consistent with our interpretation that at 397 and 494 K xenon atoms are significantly localized, whereas at 716 K they are highly mobile based on the observed changes in the distribution of the guest–host interaction energy as well as the radial distribution functions. A short trajectory of xenon at 397 and 716 K is shown in Fig. 8. It is seen that at 397 K xenon is essentially confined to the vicinity of the inner surface of the cage or the adsorption site, whereas at 716 K, xenon is considerably more delocalized. Using the Einstein relation (11)

$$D = \langle u^2(t)\rangle/2d_i t, \tag{2}$$

we have calculated the diffusion coefficients (D) at the three different temperatures, which are listed in Table 3. Here d_i is the dimensionality for the sorbate motion which we have taken as three. The diffusion coefficient values were obtained by fitting a straight line to the mean-square displacement plot over the range 25–125 ps. A plot of ln $\langle u^2(t)\rangle$ against ln t is shown in Fig. 9. A crossover from ballistic motion to diffusive motion is observed around ln $t \simeq 1$. Such a crossover has also been observed in other zeolites (7, 8, 12). The time of crossover varies between 1 and 1.2 ps, depending on the temperature.

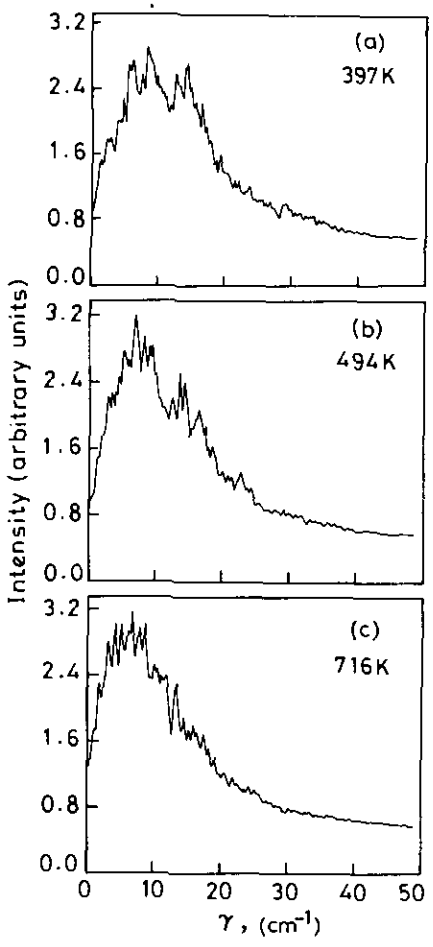

FIG. 6. Power spectra for xenon sorbed in cloverite obtained by Fourier transformation of velocity autocorrelation function at different temperatures.

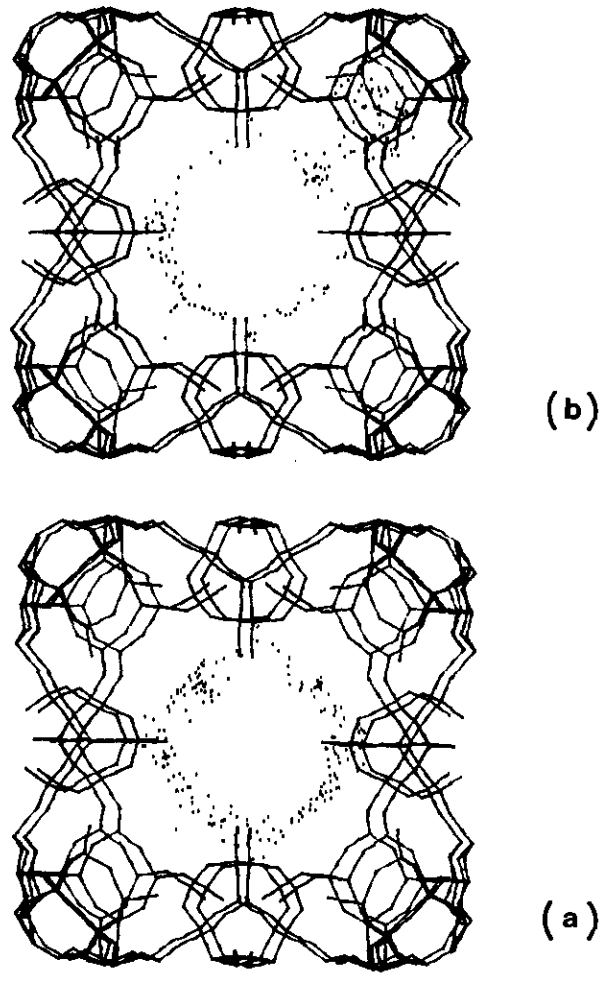

FIG. 8. Molecular dynamics trajectories of xenon sorbed in the cubic supercage of cloverite at (a) 397 and (b) 716 K.

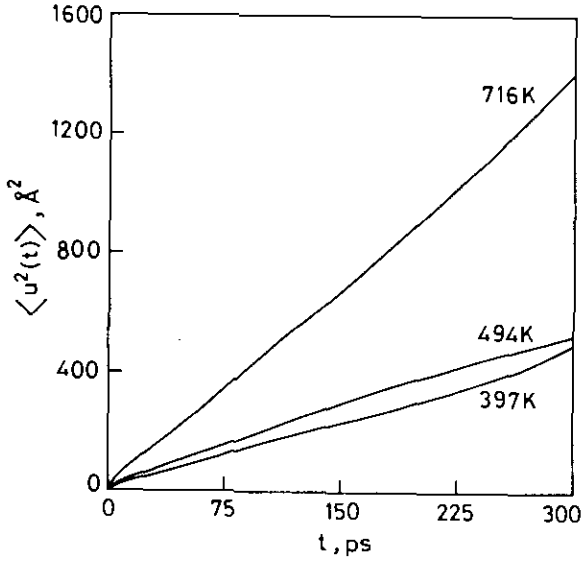

FIG. 7. A plot of average mean-square displacement with time at 397, 494, and 716 K. Xenon at 716 K is significantly more mobile.

TABLE 3

Diffusion Coefficients at Different Temperatures Obtained from Einstein's Relationship (Eq. [2]) Using the Long Time Slope of the Mean-Square Displacement after the Crossover

T(K)	397	494	716
$D \times 10^8$ (m^2/sec)	0.255	0.308	0.739

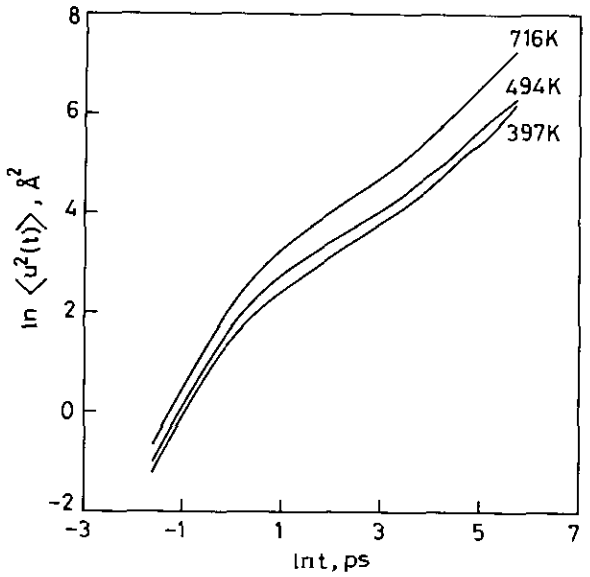

FIG. 9. A log–log plot of mean-square displacement against time. A crossover from ballistic to diffusive motion is observed around 1 ps.

5. CONCLUSIONS

Xenon is found to adsorb in the pockets located at the corners of the cubic supercage whose body diagonal is about 30 Å in length. The guest–host interaction energy at the adsorption site is −24 kJ/mole. At lower temperatures (below 500 K), xenon is relatively less mobile. By 716 K, xenon attains significantly higher mobility. Power spectra show a shift in the main peak toward lower frequency. Mean-square displacement exhibits a crossover from ballistic to diffusive motion around 1 ps.

ACKNOWLEDGMENT

One of the authors (S.B.) gratefully acknowledges the Council of Scientific and Industrial Research (C.S.I.R), New Delhi, India, for the award of a fellowship. We are happy to dedicate this work to Professor C. N. R. Rao on the occasion of his 60th birthday. One of us (S. Y.) has enjoyed long and fruitful years of collaboration with him. He has shown continued interest in our work.

REFERENCES

1. J. M. Lehn, *Science* **227,** 849 (1985).
2. C. J. Pedersen and H. K. Frensdroff, *Angew. Chem. Int. Ed. Engl.* **11,** 16 (1972).
3. J. M. Thomas, *Philos. Trans. R. Soc. London, Ser. A* **333,** 173 (1990).
4. M. Estermann, L. B. McCusker, C. Baerlocher, A. Merrouche, and H. Kessler, *Nature* **352,** 320 (1991).
5. R. L. Bedard, C. L. Bowes, N. Coombs, A. J. Holmes, T. Jiang, S. J. Kirkby, P. M. MacDonald, A. Malek, G. A. Ozin, S. Petrov, N. Plavac, R. A. Ramic, M. R. Steele, and D. Young, *J. Am. Chem. Soc.* **115,** 2300 (1993).
6. S. Yashonath, J. M. Thomas, A. K. Nowak, and A. K. Cheetham, *Nature* **331,** 601 (1988).
7. P. Santikary, S. Yashonath, and G. Ananthakrishna, *J. Phys. Chem.* **96,** 10469 (1992).
8. S. Yashonath and P. Santikary, *J. Phys. Chem.* **97,** 3849 (1993).
9. A. V. Kiselev and P. Q. Du, *J. Chem. Soc. Faraday Trans. 2* **77,** 1 (1981).
10. W. L. Jorgensen, *J. Am. Chem. Soc.* **103,** 335 (1981).
11. M. P. Allen, and D. J. Tildesley, "Computer Simulation of Liquids." Clarendon Press, Oxford, UK, 1987.
12. S. Yashonath and P. Santikary, *J. Phys. Chem.* **97,** 13778 (1993).